ACS OMEGA

http://pubs.acs.org/journal/acsodf

Article

Oxygen-Induced Elemental Mercury Oxidation in Chemical Looping Combustion of Coal

Qiuqi Liu, Dunyu Liu,* Mingguo Ni, Kailong Xu, Jingjing Ma, Zhuang Liu, Jing Jin, and Huancong Shi*

Cite This: *ACS Omega* 2022, 7, 20959−20967

Read Online

ACCESS | Metrics & More | Article Recommendations

ABSTRACT: Mercury emission is an important issue during chemical looping combustion (CLC) of coal. The aim of this work is to explore the effects of different flue gas components (e.g., HCl, NO, SO_2, and CO_2) on mercury transformation in the flue gas cooling process. A two-stage simulation method is used to reveal the reaction mechanism of these gases affecting elemental mercury (Hg^0) oxidation. Furthermore, using this method, Hg^0 oxidation by eight oxygen carriers (Co_3O_4, $CaSO_4$, CeO_2, Fe_2O_3, Al_2O_3, Mn_2O_3, SiO_2, and CuO) commonly used in CLC are investigated and their Hg^0 oxidation efficiencies were compared with the existing experimental results. The results show that HCl, NO, and CO_2 promote Hg^0 oxidation during flue gas cooling, while SO_2 inhibits Hg^0 oxidation. The stronger the oxygen release capacity of oxygen carriers, the higher the oxidation efficiency of Hg^0 becomes. The order of Hg^0 removal efficiency from high to low is Co_3O_4, CuO, Mn_2O_3, $CaSO_4$, Fe_2O_3, CeO_2, Al_2O_3, and SiO_2, and this sequence is in good agreement with the existing experimental results. Different flue gas components directly or indirectly affect the O_2 content, thus affecting the content of gaseous oxidized mercury (Hg^{2+}). Different oxygen carriers have different oxygen release capacities and different Hg^0 oxidation efficiencies. Therefore, O_2 is the core species affecting the mercury transformation in CLC.

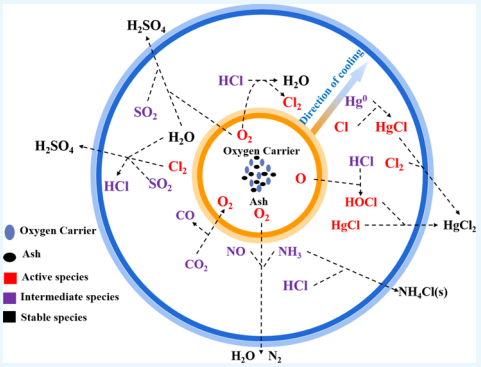

1. INTRODUCTION

One of the biggest challenges facing the world today is global warming. Coal combustion produces a large amount of carbon dioxide, which is the main reason for the greenhouse effect in the atmosphere. To mitigate climate change, CO_2 emission control and carbon capture utilization and storage (CCUS) are potentially viable approaches and promising options to alleviate increasing carbon dioxide (CO_2) emissions in human society.[1−3] China's energy structure of rich coal, poor oil, and little gas determines that coal will occupy an important energy position for a long time. However, coal combustion releases a large amount of trace element mercury. Generally speaking, mercury in coal-fired flue gas mainly exists in three forms: elemental mercury (Hg^0), oxidized mercury (Hg^{2+}), and particle-bound mercury (Hg^P).[4,5] Among them, Hg^{2+} is easily soluble in water and can be removed using a wet flue gas desulfurization device,[6] Hg^P generally exists on the surface of solid particles such as fly ash and can be removed using an electrostatic precipitator or a bag filter,[7] and Hg^0 is volatile and insoluble in water, so it is difficult to be effectively removed using the existing flue gas purification equipment.[8,9] Considering the high toxicity, mobility, and bioaccumulation of Hg^0, it is necessary to effectively treat Hg^0 produced in the combustion process.[10,11]

Among the carbon capture technologies, chemical looping combustion (CLC) has recently emerged as a promising option to facilitate CO_2 inherent separation at a low cost. It is a new combustion technology containing a circulating combustion system composed of an air reactor (AR) and a fuel reactor (FR).[3] Different from the traditional combustion mode, the oxygen required in CLC is not directly provided by air, but by the oxygen carrier (OC). OC circulates between FR and AR to realize its reduction and regeneration.[12] Therefore, the core of CLC is to select appropriate OC, which can not only provide lattice oxygen[13,14] but also catalyze the oxidation of Hg^0 released by coal combustion and effectively reduce the emission of Hg^0.[15]

The reactor temperature of CLC is about 800−1000 °C. It is generally considered that when the temperature is higher than 800 °C, the mercury species mainly exist as Hg^0. When the temperature is reduced to 700 °C, part of Hg^0 will be oxidized to Hg^{2+}. Mendiara et al. used Fe_2O_3 as OC to study the mercury release in CLC.[16,17] It was found that the fraction of the mercury in coal vaporized in the FR mainly depended on the temperature of the FR and the coal used. At the same time, the species of mercury was measured. It was found that Hg^0

Received: March 21, 2022
Accepted: May 13, 2022
Published: June 6, 2022

ACS Publications

© 2022 The Authors. Published by American Chemical Society

Table 1. Initial Quantity of Each Substance in the Thermodynamic System

species	C	H	O	N	S	Cl	N_2	H_2O	Hg
n/mol	0.634	0.350	0.01	0.0021	0.00137	6.58×10^{-6}	0.89	0.89	1.26×10^{-8}

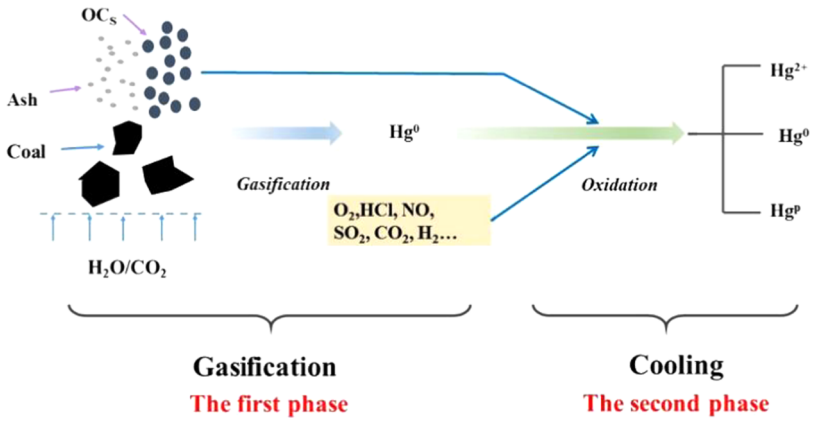

Figure 1. Two-stage simulation method.

was the main species in the FR. Pérez-Vega et al. used CuO as the OC, and it was found that owing to the presence of copper oxide as the oxygen carrier, which has oxygen uncoupling ability, the volatilized Hg was further oxidized to Hg^{2+}.[18] Ma et al. found that in the presence of hematite in the FR, the concentration of Hg^0 decreased and the concentration of Hg^{2+} increased, indicating that hematite promoted the conversion of Hg^0 to Hg^{2+}.[19] Only a small amount of mercury was adsorbed by the OC and transported to the AR together with the carbon residue, which was released in the form of $Hg^0(g)$ and $Hg^{2+}(g)$ or left in OC and coal ash in the form of Hg^p. Ji et al. used ferrous ore as OC to study the release characteristics of mercury in bituminous coal in CLC. It was found that most of the mercury in coal was released in FR, and the rest was released in AR. In particular, Hg^0 is the main species of released mercury.[20] However, with the increase of FR temperature, the amount of Hg^0 may decrease and the amount of Hg^{2+} may increase. This can be attributed to different flue gas components.[21,22]

At present, the mechanism of Hg^0 oxidation by oxygen carriers in the furnace has been reported,[23] but the effects of flue gas components produced in the gasification process on mercury transformation in the cooling stage are not clear. Certainly, oxygen carriers may have a significant influence on Hg^0 oxidation through the coal gasification process. In the CLC process, coal-fired flue gas contains many gas components such as Cl_2, HCl, SO_2, and CO. According to early studies, the presence of Cl_2/HCl in flue gas is the main reason for the migration and transformation of mercury,[24] and Hg^0 oxidation reactions occur during flue gas cooling.[25] However, the actual flue gas is too complex and the mechanism by which these flue gas components affect Hg^0 oxidation is not yet clear.

In this paper, we propose a two-stage simulation method to understand the effects of oxygen carriers on the gasification process, and the effects of gas components produced in the gasification process on the transformation of mercury in the flue gas cooling stage. The reaction paths are potentially revealed. The Hg^0 oxidation efficiencies of OCs in FR are simulated and compared with the experimental results. This paper provides a theoretical basis for simulating the mercury transformation mechanism in CLC, and also provides a technical method for the selection of oxygen carriers with Hg^0 oxidation ability.

2. RANKING METHOD

2.1. Thermodynamic Simulation. To evaluate Hg^0 oxidation efficiencies of different OCs, the speciation of mercury in the system should be calculated. Therefore, a thermodynamic calculation was performed by the Equilib module in FactSage 5.2. Chemical equilibrium calculation is performed by means of a general Gibbs energy minimization algorithm. The Equilib module calculates the conditions for multiphase, multicomponent equilibria, with a wide variety of tabular and graphical output modes, under a large range of possible constraints through Gibbs energy minimization based on the ChemApp algorithm.[26]

When the chemical equilibrium is investigated, the standard Gibbs free energy change (ΔG) of the reaction is often used. A possible way to determine whether some specific chemical processes can occur spontaneously is by calculating the ΔG energy of the reaction. The definition of ΔG can be given by eq 1.

$$\Delta G = \Delta H - T\Delta S \quad (1)$$

where ΔH is the enthalpy, T is the absolute temperature, and ΔS is the entropy.

According to eq 1, there are three possibilities for ΔG in any process, namely:

$\Delta G < 0$: the reaction is likely to proceed spontaneously without involving external energy.

$\Delta G = 0$: the chemical reaction is at a thermodynamic equilibrium.

$\Delta G > 0$: the possibility of the reaction to proceed spontaneously without external energy is very small.

The priority of thermodynamic simulation is to predict Hg^0 oxidation efficiency. However, the methodology has not been established. Our previous research proposed that Cl_2 generated in the "Hg^0 + HCl + Me_xO_y" system can be used to rank the ability of different oxygen carriers for Hg^0 oxidation.[23] However, Hg^0 oxidation efficiency cannot be predicted for different systems containing different oxygen carriers. On top

https://doi.org/10.1021/acsomega.2c01709
ACS Omega 2022, 7, 20959−20967

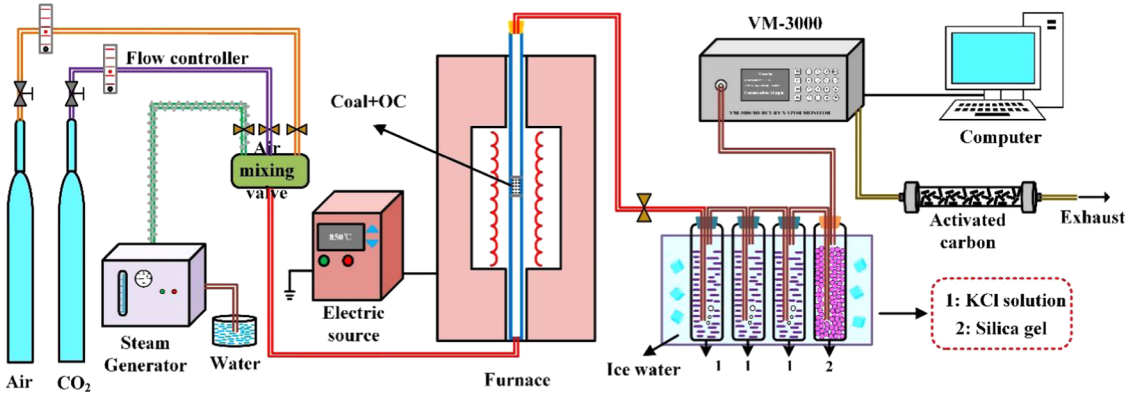

Figure 2. CLC experimental system.

of our previous research, our aim is to establish a methodology for the calculation of Hg^0 oxidation efficiency.

The typical experimental results obtained by An et al. were chosen for the development of the simulation methodology. According to the previous results obtained in a fluidized bed using $CuFe_2O_4$ as the oxygen carrier to oxidize Hg^0, it is found that when 1 L/min (STP) gas flow (N_2/H_2O = 50/50%) was used as the gasification atmosphere, the Hg^0 proportion with respect to total mercury measured at the tail gas outlet after 40 min was 60.92%.[27] Thermodynamic simulation is attempted to match this result.

The initial conditions for simulation are taken from the paper published by An et al. High mercury-containing lignite (YN) was used in the simulation, and the elements contained in YN mainly included C, H, O, N, S, Cl, and Hg.[27] The gasification atmosphere was N_2 and H_2O. The oxygen carrier was $CuFe_2O_4$, and the experimental temperature was 850 °C. In the experiment, 10 g YN and 1 L/min (STP) gas flow (N_2/H_2O = 50/50%) were used. Thus the initial amount of these substances in the simulation is shown in Table 1.

By observing the experimental system published previously, two stages may be involved, as shown in Figure 1. The first stage is the coal gasification process which occurs in the furnace. The second stage is the cooling stage which occurs outside the furnace and before analysis. In this stage, the flue gas after coal gasification, which comes out of the furnace passes through the ice bath and then enters the mercury analyzer. Both processes are simulated using the Equilib module in FactSage. The Reaction module in the thermodynamic calculation software FactSage is used to calculate Gibbs free energy change (ΔG).

The gasification process of coal and $CuFe_2O_4$ under a N_2 and H_2O atmosphere is first simulated, and then the gasification products of this process are taken as the reactants in the second stage to continue to simulate mercury transformation during cooling.

2.2. Experimental Apparatus. Experiments were carried out in a drop furnace. In the experiments, eight oxygen carriers, including $CaSO_4$, Co_3O_4, Mn_2O_3, Fe_2O_3, CuO, CeO_2, SiO_2, and Al_2O_3 were adopted. These eight substances were acquired from Sinopharm Chemical Reagent Co., Ltd. Zhundong coal was used in the experiment, and it had a fine grain of 80−100 mesh.

As can be observed from Figure 2, the experimental setup was composed of five main parts: the gas feed system, coal gasification section, gas cooling section, analysis instrument for Hg^0 (VM3000, mercury analyzer), and the exhaust gas treatment device (with activated carbon). Approximately 5 g of Zhundong coal and oxygen carriers with different contents were packed into the drop furnace in each experiment. The total amount of mercury was about 0.7 μg. The temperature of the reactor was controlled at 850 °C. In the reduction reactor, the CO_2 flow rate was 5 L/min and the H_2O flow rate was 1 L/min. The four impact bottles in the gas cooling section were respectively filled with 1 mol/L KCl solution and silica gel particles. KCl solution was mainly used to absorb Hg^{2+} in gas. Silica gel particles were used to remove moisture in gas and to prevent moisture from entering VM3000 and damaging the instrument.

3. RESULTS AND DISCUSSION

3.1. Validation of the Simulation Method. In the first step of the simulation, the only uncertainty is the initial content of $CuFe_2O_4$. To determine the content of $CuFe_2O_4$, different contents of oxygen carriers are optimized in the calculation. In the experiment, the gasification products first passed through the ice bath and then entered the mercury analyzer. Therefore, the gas temperature entering the mercury analyzer was about 0−10 °C. In the $CuFe_2O_4$ system with different quantities, the gasification process of coal and $CuFe_2O_4$ under a N_2 and H_2O atmosphere is first simulated, and the gasification product of this process is then taken as the reactant in the second stage to simulate mercury transformation in the cooling process. Finally, the proportion of Hg^0 at 0−10 °C can be obtained by the thermodynamic method. The proportion of Hg^0 in the $CuFe_2O_4$ system with different contents can be obtained by averaging the proportion of Hg^0 at 0 and 10 °C.

As shown in Figure 3, when the amount of OC is 2−3 mol, the proportion of Hg^0 decreases significantly. Therefore, an optimal value is selected in this interval to make the proportion of Hg^0 consistent with the experimental results of An et al. (60.92%).[27] The calculation results of the first stage show that the gas components after gasification contain mainly CO_2, SO_2, H_2, CO, HCl, NO, O_2, etc.

The second process is the cooling of the gasification product. Sliger et al. investigated the homogeneous oxidation of chlorine and mercury by the kinetic model. They believe that the Hg^0 oxidation occurs in the cooling process of flue gas.[25] According to the thermodynamic results, Hg^{2+} mainly exists in three forms $HgCl_2$, HgS, and HgO. Since the amount of total mercury is small, it is only 1.26×10^{-8} mol, and in addition, the main mercury species in the second stage are Hg^0 and $HgCl_2$. Therefore, the amount of $HgCl_2$ is mainly used as

https://doi.org/10.1021/acsomega.2c01709
ACS Omega 2022, 7, 20959−20967

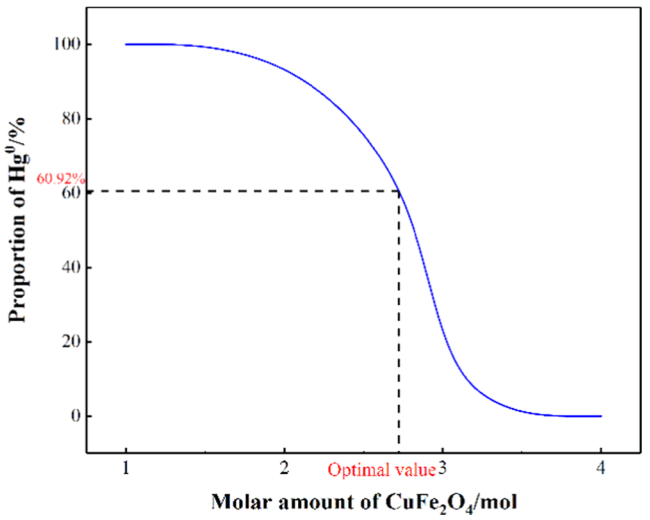

Figure 3. Effect of the OC amount on the proportion of Hg^0.

the evaluation standard of the Hg^0 oxidation efficiency. In the following part, we specifically discuss the impact of different flue gas components on Hg^0 oxidation in this system.

3.2. Influence of Gas Compositions. To explore the influence of different flue gas components on Hg^0 oxidation in the flue gas cooling process, sensitivity analysis of HCl, NO, H_2, CO, SO_2, and CO_2 was carried out. Seven working conditions including "All," "Remove HCl," "Remove NO," "Remove SO_2," "Remove CO_2," "Remove H_2," and "Remove CO" were designed. "All" represents the case with all the gasification species included, whereas "Remove gas" represents the case with all the gasification species except for the indicated gas. It is found that in the cooling process from 800 °C to 0 °C, H_2 and CO have little impact on Hg^0 oxidation, while HCl, NO, SO_2, and CO_2 have different degrees of impact on Hg^0 oxidation at different temperatures as shown in Figure 4. Therefore, next, we mainly discuss how these four gases affect Hg^0 oxidation.

As can be seen from Figure 4a, when HCl is removed, the amount of $HgCl_2$ in the whole process is reduced. Therefore, HCl promotes Hg^0 oxidation in the whole temperature range. For NO, the effect is not obvious in the range of 100−800 °C. In the range of 0−100 °C, when NO is removed, $HgCl_2$ is reduced, and thus NO plays a promoting role. After SO_2 is removed, $HgCl_2$ increases significantly when the temperature is lower than 400 °C. Therefore, SO_2 has an obvious inhibitory effect on Hg^0 oxidation in this temperature range. When CO_2 is removed and the flue gas is cooled down from 400 to 300 °C, $HgCl_2$ decreases. Therefore, CO_2 gas is conducive to the oxidation of Hg^0 in the temperature range of 300−400 °C.

3.2.1. Effect of HCl. Since HCl is conducive to the oxidation of Hg^0 in the whole temperature range, to see more clearly how HCl affects the amount of $HgCl_2$, 300 °C is taken as the discussion temperature. Comparing "All" and "Remove HCl" systems, the main substances which are changed include HCl, $HgCl_2$, Cl_2, Cl, and HOCl as shown in Table 2. When HCl is present, the amounts of HCl, Cl_2, Cl, and HOCl increase, resulting in an increased Hg^0 oxidation efficiency.

For HCl, the increase in the amounts of HCl, Cl_2, Cl, and HOCl is the key to the increased Hg^0 oxidation efficiency. The Gibbs free energy change (ΔG) for the reactions related to the conversion of Hg^0 to $HgCl_2$ in the "All" system are calculated.

The reaction pathways of HCl related reactions to generate Cl_2, Cl, and HOCl are shown in R1−R3 in Table 3. The global reaction for the direct oxidation of Hg^0 by HCl is R4. Due to the high energy barrier of the direct reaction between Hg^0 and HCl, it is calculated as $\Delta G > 0$ at 300 °C. This is consistent with previous results of Wilcox et al.[28] Widmer et al. proposed eight elementary reactions for mercury oxidation including R5−R12.[29] It is calculated that R5, R9, R10, and R11 are the main reactions for Hg^0 oxidation in the "All" system. The reaction pathway may be described as follows. Hg^0 is oxidized to HgCl (R5), and then HgCl reacts with Cl_2, Cl, and HOCl to form $HgCl_2$ (R9−R11).

3.2.2. Effect of NO. Because NO is conducive to Hg^0 oxidation in the range of 0−100 °C, it is studied separately. Figure 5 shows that the amounts of $HgCl_2$ in the two systems are similar in the temperature range of 70−100°C. When the temperature is lower than 70 °C, the amount of $HgCl_2$ in the "Remove NO" system decreases rapidly. Therefore, NO is conducive to Hg^0 oxidation within 0−70 °C. To more clearly compare the changes in the amount of substances of each

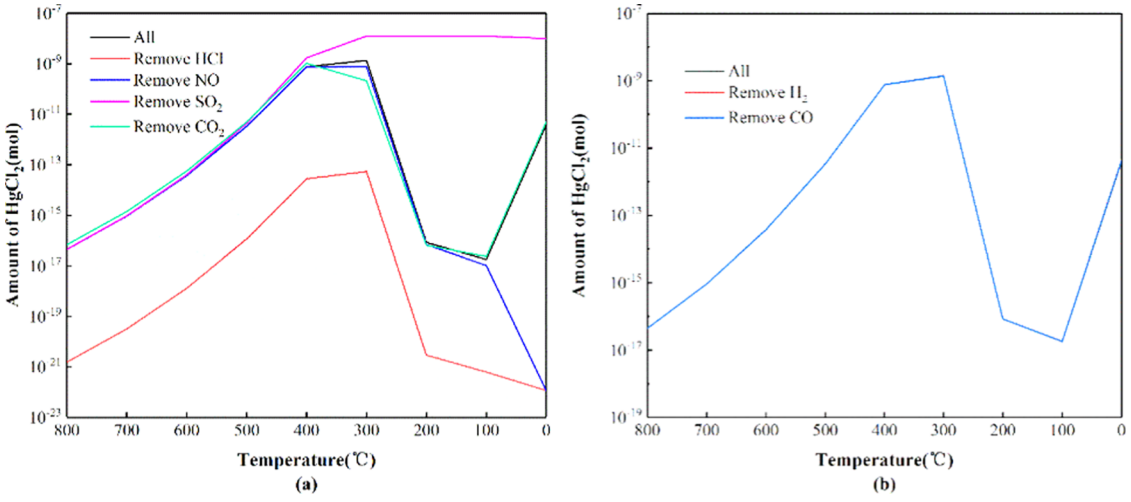

Figure 4. Variation of $HgCl_2$ with temperature under seven working conditions: (a) "All" is compared with "Remove HCl", "Remove NO", "Remove SO_2", and "Remove CO_2" and (b) "All" is compared with "Remove H_2" and "Remove CO".

https://doi.org/10.1021/acsomega.2c01709
ACS Omega 2022, 7, 20959−20967

Table 2. Amount of Different Species at 300 °C in "All" and "Remove HCl" Systems

species	n/mol		species	n/mol	
	All	Remove HCl		All	Remove HCl
H_2O	1.06	1.06	O_2	2.63×10^{-11}	2.63×10^{-11}
N_2	0.89	0.89	NO	1.28×10^{-13}	1.28×10^{-13}
CO_2	6.34×10^{-1}	6.34×10^{-1}	HgO	2.08×10^{-14}	2.33×10^{-14}
SO_2	7.91×10^{-6}	7.91×10^{-6}	Cl_2	8.47×10^{-15}	2.93×10^{-19}
HCl	6.58×10^{-6}	3.87×10^{-8}	H_2	7.72×10^{-15}	7.72×10^{-15}
$O_2S(OH)_2$	2.36×10^{-6}	2.36×10^{-6}	Cl	9.08×10^{-16}	5.35×10^{-18}
SO_3	3.13×10^{-7}	3.13×10^{-7}	OH	8.46×10^{-16}	8.46×10^{-16}
Hg	1.12×10^{-8}	1.26×10^{-8}	HOCl	7.76×10^{-16}	4.57×10^{-18}
$HgCl_2$	1.37×10^{-9}	5.34×10^{-14}	CO	1.12×10^{-16}	1.12×10^{-16}

Table 3. Gibbs Free Energy Change of Each Reaction at 300 °C

number	reaction	ΔG (kJ mol^{-1})	number	reaction	ΔG (kJ mol^{-1})
R1	$2HCl + 0.5O_2 = Cl_2 + H_2O$	−19.87	R2	$HCl + OH = Cl + H_2O$	−57.46
R3	$HCl + O = HOCl$	−166.39	R4	$Hg^0 + 2HCl = HgCl_2 + H_2$	46.62
R5	$Hg^0 + Cl = HgCl$	−57.74	R6	$Hg^0 + Cl_2 = HgCl + Cl$	122.47
R7	$Hg^0 + HOCl = HgCl + OH$	111.42	R8	$Hg^0 + HCl = HgCl + H$	319.25
R9	$HgCl + Cl_2 = HgCl_2 + Cl$	−91.18	R10	$HgCl + Cl = HgCl_2$	−271.39
R11	$HgCl + HOCl = HgCl_2 + OH$	−102.24	R12	$HgCl + HCl = HgCl_2 + H$	105.59
R13	$SO_2 + 0.5O_2 + H_2O = H_2SO_4$	−159.38	R14	$SO_2 + Cl_2 + 2H_2O = 2HCl + H_2SO_4$	−295.92
R15	$SO_2 + 0.5O_2 = SO_3$	−44.91	R16	$SO_3 + H_2 = SO_2 + H_2O$	−170.50
R17	$N_2 + O_2 = 2NO$	166.32	R18	$CO_2 = 0.5O_2 + CO$	233.16

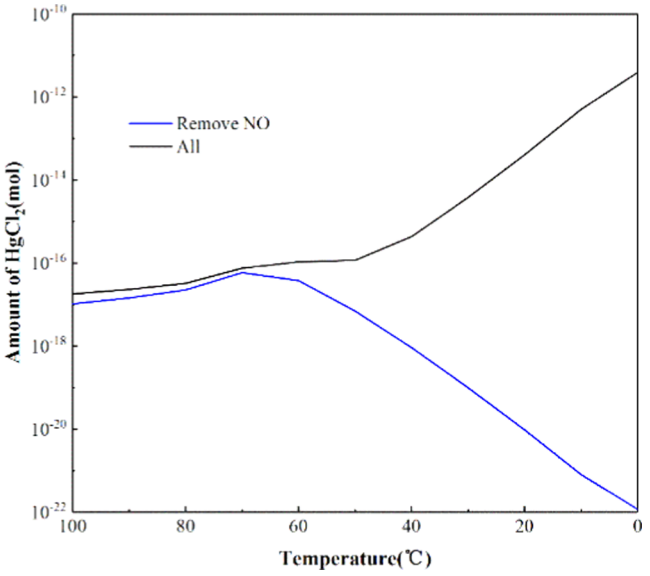

Figure 5. Amount of $HgCl_2$ changes with temperature for "All" and "Remove NO" systems.

species in two systems, 30 °C is taken as the investigation temperature.

Table 4 shows that NO most directly affects the amount of NH_3 and NH_4Cl (s). Compared with the "Remove NO" system, NH_3 and NH_4Cl (s) in the "All" system decrease. Similarly, gases including H_2, CH_4, CO, and $HgCl_2$ decrease, while HCl and CuCl(s) increase.

As given in Table 5, NO in "All" system directly affects the amounts of NH_3 and NH_4Cl (s) through R19 and R20. In detail, NO consumes a large amount of NH_3 to produce N_2 and H_2O (R19). However, the amounts of N_2 and H_2O are much greater than that of NO, the increase of N_2 and H_2O cannot be clearly observed in the calculation results. Therefore, after NH_3 is consumed, NH_4Cl (s) produced by the reaction of NH_3 with HCl decreases (R20). At the same time, $HgCl_2$ increases as more HCl is involved in the oxidation of Hg^0 rather than reacting with NH_3. The reduction of CO and H_2 may be due to the reaction with O_2 to produce CO_2 and H_2O (R21 and R22). When CO and H_2 are consumed, the generated CH_4 decreases (R23).

3.2.3. Effect of SO_2. Since the amount of $HgCl_2$ in the "Remove SO_2" system tends to be stable at temperatures below 300 °C, and it is taken as the investigation temperature. In comparison with the "Remove SO_2" system, in the "All"

Table 4. Amount of Different Species at 30 °C in "All" and "Remove NO" Systems

species	n/mol		species	n/mol	
	All	Remove NO		All	Remove NO
N_2	8.91×10^{-1}	8.91×10^{-1}	NH_3	4.32×10^{-10}	2.25×10^{-8}
CO_2	6.34×10^{-1}	6.34×10^{-1}	CH_4	3.15×10^{-11}	1.19×10^{-6}
H_2O	6.68×10^{-2}	6.68×10^{-2}	CO	1.43×10^{-12}	1.99×10^{-11}
HCl	1.29×10^{-6}	2.48×10^{-8}	$HgCl_2$	3.77×10^{-15}	9.97×10^{-12}
Hg	1.26×10^{-8}	1.26×10^{-8}	NH_4Cl(s)	5.25×10^{-6}	6.56×10^{-6}
H_2	1.20×10^{-8}	1.68×10^{-7}	CuCl(s)	3.78×10^{-8}	0

https://doi.org/10.1021/acsomega.2c01709
ACS Omega 2022, 7, 20959−20967

Table 5. Gibbs Free Energy Change of Each Reaction at 30 °C

number	reaction	ΔG (kJ mol^{-1})	number	reaction	ΔG (kJ mol^{-1})
R19	$4NO + 4NH_3 + 2O_2 = 4N_2 + 6H_2O$	−1628.44	R20	$NH_3 + HCl = NH_4Cl(s)$	−177.03
R21	$CO + 0.5O_2 = CO_2$	−256.84	R22	$H_2 + 0.5O_2 = H_2O$	−228.38
R23	$CO + 3H_2 = CH_4 + H_2O$	−149.18			

Table 6. Amounts of Some Species at 300 °C in "All" and "Remove SO_2" Systems

	n/mol			n/mol	
species	All	Remove SO_2	species	All	Remove SO_2
H_2O	1.06	1.06	$HgCl_2$	1.37×10^{-9}	1.26×10^{-8}
N_2	0.89	0.89	O_2	2.63×10^{-11}	6.76×10^{-4}
CO_2	6.34×10^{-1}	6.34×10^{-1}	NO	1.28×10^{-13}	6.47×10^{-10}
SO_2	7.91×10^{-6}	1.52×10^{-9}	HgO	2.08×10^{-14}	1.94×10^{-13}
HCl	6.58×10^{-6}	6.55×10^{-6}	Cl_2	8.47×10^{-15}	4.22×10^{-11}
$O_2S(OH)_2$	2.36×10^{-6}	2.30×10^{-6}	H_2	7.72×10^{-15}	1.54×10^{-18}
SO_3	3.13×10^{-7}	3.03×10^{-7}	Cl	9.08×10^{-16}	6.42×10^{-14}
Hg	1.12×10^{-8}	2.07×10^{-11}	$H_2SO_4(H_2O)_6$(liq)	1.36×10^{-3}	8.39×10^{-6}

Table 7. Amount of Some Species at 300 °C in "All" and "Remove CO_2" Systems

	n/mol			n/mol	
species	All	Remove CO_2	species	All	Remove CO_2
H_2O	1.06	1.06	O_2	2.63×10^{-11}	2.18×10^{-13}
N_2	0.89	0.89	NO	1.28×10^{-13}	1.16×10^{-14}
CO_2	6.34×10^{-1}	9.70×10^{-8}	HgO	2.08×10^{-14}	2.41×10^{-15}
SO_2	7.91×10^{-6}	7.91×10^{-6}	Cl_2	8.47×10^{-15}	8.89×10^{-16}
HCl	6.58×10^{-6}	6.58×10^{-6}	H_2	7.72×10^{-15}	7.36×10^{-14}
$O_2S(OH)_2$	2.36×10^{-6}	3.28×10^{-7}	Cl	9.08×10^{-16}	2.56×10^{-16}
SO_3	3.13×10^{-7}	3.28×10^{-8}	OH	8.46×10^{-16}	2.38×10^{-16}
Hg	1.12×10^{-8}	1.24×10^{-8}	HOCl	7.76×10^{-16}	8.14×10^{-17}
$HgCl_2$	1.37×10^{-9}	2.11×10^{-10}	CO	1.12×10^{-16}	1.63×10^{-22}

system, the quantities of SO_2, SO_3, $O_2S(OH)_2$, $H_2SO_4(H_2O)_6$(liq), HCl, and H_2 increase, while $HgCl_2$, O_2, NO, HgO, Cl_2, and Cl decrease as seen in Table 6.

In the system where SO_2 exists, the amount of SO_2 increases, and then O_2 is consumed to generate H_2SO_4 (R13), resulting in the increase of $H_2SO_4(H_2O)_6$(liq). Meanwhile, the higher concentration of SO_2 in the flue gas will also react with Cl_2 and H_2O to produce HCl and H_2SO_4 (R14). Therefore, Cl/Cl_2 decreases and HCl increases. However, according to the above analysis, Hg^0 cannot directly react with HCl to produce $HgCl_2$. Therefore, the presence of SO_2 consumes Cl and Cl_2, which is the main reason for the reduction of the Hg^0 oxidation efficiency. The increase of SO_3 is due to the oxidation of SO_2 by O_2 (R15). In "Remove SO_2," the amount of SO_3 is more than that of SO_2, so SO_3 reacts with H_2 to produce SO_2 and H_2O (R16). In the system where SO_2 exists, the amount of SO_2 is more than that of SO_3, so SO_2 consumes O_2 to produce SO_3 (R15). Under such a circumstance, H_2 is not consumed, and therefore, the amount of H_2 increases.

3.2.4. Effect of CO_2. For CO_2, it is conducive to Hg^0 oxidation in the range of 300−400 °C. Thus 300 °C is taken as the investigation temperature. Table 7 shows that the CO_2, O_2, and CO gases in the "All" system increase, as well as $HgCl_2$, HgO, $O_2S(OH)_2$, SO_3, NO, Cl_2, Cl, and HOCl. Since the amount of CO_2 is 0.634mol, accounting for a large part of the whole system, the overall C and O will be greatly reduced after CO_2 is removed. On the contrary, in the presence of CO_2, O_2 and CO also increase, and the increase of O_2 leads to the increase of HgO. At the same time, the increased O_2 reacts with HCl to produce Cl_2 (R1), which eventually leads to the increase of $HgCl_2$. It can be seen that the addition of CO_2 leads to the increase of O_2, which is the key to the improvement of Hg^0 oxidation efficiency. The increase of O_2 lead to the increase of Cl_2, Cl, HOCl, SO_3, and NO (R1−R3, R15, and R17).

3.3. Effects of Different Oxygen Carriers. This part aims to analyze the Hg^0 removal performance of common oxygen carriers in CLC using the simulation method discussed previously. Considering that the O element in the OC can promote the oxidation of Hg^0, the oxygen content of other oxygen carriers will be controlled to provide the same amount of oxygen atoms. By comparing the Hg^0 oxidation efficiency of eight oxygen carrier systems, the order of Hg^0 removal performance of oxygen carriers can be obtained. The order of Hg^0 removal efficiency from high to low is Co_3O_4, CuO, Mn_2O_3, $CaSO_4$, Fe_2O_3, CeO_2, Al_2O_3, and SiO_2.

In the process of CLC, due to the addition of different oxygen carriers, the reactions will be different. Therefore, the gasification products in this process will also be different. It is well known that the conversion of Hg^0 to Hg^{2+} depends largely on these gases. According to the first stage simulation, the gases produced in the gasification process mainly include CO_2, SO_2, H_2, CO, HCl, NO, and O_2. Among these gas components, the content of O_2 is closely related to the Hg^0 removal efficiency. In Co_3O_4 and CuO systems, with relatively high oxygen content, their Hg^0 removal efficiency is high. At the same time, due to the different content of O_2, the amount of Cl and Cl_2 produced by the homogeneous reaction is also

https://doi.org/10.1021/acsomega.2c01709
ACS Omega 2022, 7, 20959−20967

different. It can be found from Figure 6 that the oxidation efficiency of Hg^0 is directly related to the amount of O_2, Cl, and Cl_2.

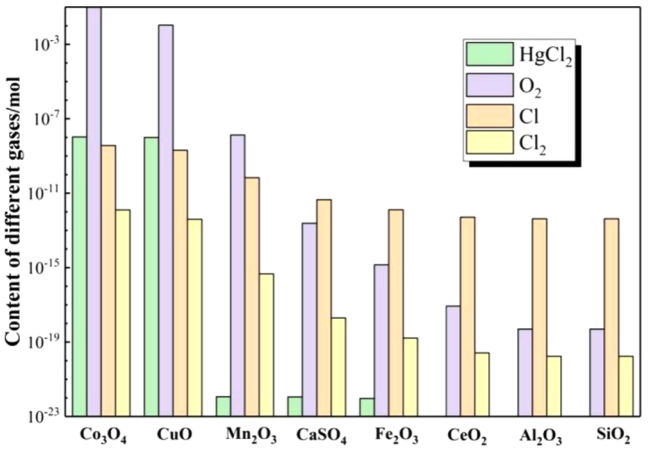

Figure 6. Amount of gasification components of each system.

In our existing experiments, the order of Hg^0 removal efficiency from high to low is Co_3O_4 > Mn_2O_3 > Fe_2O_3 > CuO > $CaSO_4$ > CeO_2 > SiO_2 > Al_2O_3. The proportions of Hg^0 and Hg^{2+} released with respect to total mercury were 5.01, 6.34, 6.46, 9.66, 33.7, 68.99, 75.96, and 91.24%, respectively. As shown in Figure 7, the concentrations of Hg^0 and Hg^{2+} were

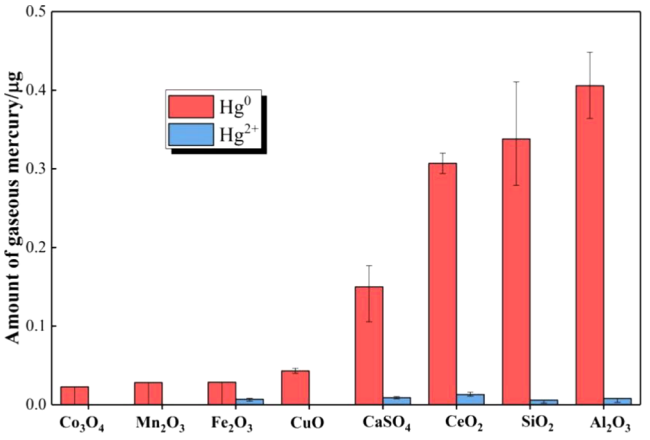

Figure 7. Total amount of gaseous mercury.

integrated to find the total amount of gaseous mercury released during the experiment, the less elemental mercury was released, the more oxidized mercury was produced. It can be found that there is a difference between the experiment and the simulation, because the simulation only considers the gas interaction in the cooling process, but does not consider the conversion of mercury by OC itself. Both homogeneous and heterogeneous reaction pathways are important for Hg^0 removal. OC can promote the conversion of Hg^0 to Hg^{2+}/Hg^P. Pérez-Vega et al. used CuO as OC and found that Hg^P accounted for 59.4% of the total Hg.[18] It was reported that mercury on OC (Co_3O_4@TiO_2@Fe_2O_3) was mainly desorbed in the form of HgO, which was beneficial for mercury removal.[15] It was found that 24.14% of the mercury in the coal migrated to the OC ($CuFe_2O_4$) with the forms of Hg^0, HgO, and $HgCl_2$ in CLG.[27] Ma et al. analyzed the mercury on the oxidized OC (CuO@TiO_2-Al_2O_3) by X-ray photoelectron spectra (XPS). XPS spectra over the spectral regions of Hg 4f were evaluated, and $HgCl_2$, HgO, HgS, and Hg^0 were detected.[13] Therefore, the heterogeneous reaction between mercury and OC needs a further in-depth study.

3.5. O_2-Induced Hg^0 Oxidation. From the discussion in previous sections, it can be found that different gas components affect the content of O_2, thus indirectly affecting the oxidation efficiency of Hg^0. As shown in Figure 8, O_2 is in

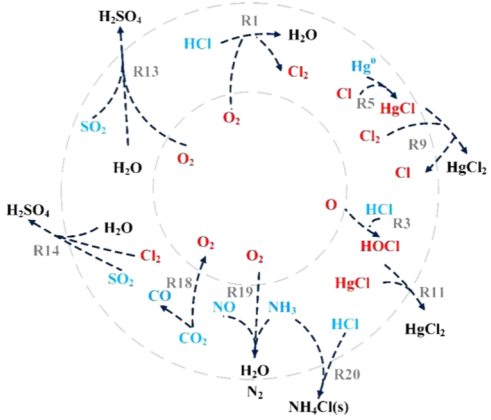

Figure 8. O_2-induced Hg^0 oxidation in chemical looping combustion.

the core position, around which are different flue gas components, and the outermost ones are the stable species. In addition to O_2, Cl, Cl_2, HOCl, and HgCl are also more active gas components. For example, the presence of HCl consumes O_2 and generates Cl_2, which results in an increase in the amount of $HgCl_2$; NO indirectly affects HCl as NH_3 and consumes O_2; the presence of SO_2 also consumes O_2 first, and then Cl_2 and Cl, so it can inhibit the Hg^0 oxidation; the amount of CO_2 is large, and it can decompose into O_2 at a certain temperature, so as to promote Hg^0 oxidation.

It can be seen from the above discussion that different oxygen carriers affect the Hg^0 oxidation efficiency, which is closely related to O_2. The stronger the oxygen release capacity of oxygen carriers, the higher the oxidation efficiency of Hg^0. Moreover, the oxygen carrier with stronger oxygen release is also conducive to combustion, which is more suitable for CLC.

4. CONCLUSIONS

A two-stage simulation method is used in this paper. The first stage is the gasification process of coal and the oxygen carrier, and then the gasification products of this process are used as the reactants in the second stage. The thermodynamic method is used to simulate the transformation of mercury in the cooling process. The simulation results are in good agreement with the experimental results, indicating that this method is reliable.

In the flue gas cooling process, HCl, NO, and CO_2 contribute to the transformation of mercury, and SO_2 inhibits Hg^0 oxidation. HCl reacts with O_2 to form Cl/HOCl, which oxidizes HgCl to $HgCl_2$, thus promoting Hg^0 oxidation; the presence of NO indirectly affects the content of HCl, resulting in more HCl participating in Hg^0 oxidation; a large amount of CO_2 decomposes into O_2 and reacts with HCl to promote Hg^0 oxidation; SO_2 consumes O_2 and Cl_2, and inhibits Hg^0 oxidation.

https://doi.org/10.1021/acsomega.2c01709
ACS Omega 2022, 7, 20959−20967

By comparing the Hg^0 oxidation efficiency of eight oxygen carrier systems, the order of Hg^0 removal efficiency from high to low is Co_3O_4, CuO, Mn_2O_3, $CaSO_4$, Fe_2O_3, CeO_2, Al_2O_3, and SiO_2, and the O_2 content in gasification products in these systems is also in this order.

Different flue gas components directly or indirectly affect the O_2 content, through which the Hg^{2+} content is affected. Different oxygen carriers have different oxygen release capacities and different Hg^0 removal effects. Therefore, O_2 is the core affecting Hg^0 transformation. The selection of oxygen carriers with strong oxygen release is more conducive to the removal of Hg^0 in chemical looping combustion.

AUTHOR INFORMATION

Corresponding Authors

Dunyu Liu − *School of Energy and Power Engineering, University of Shanghai for Science and Technology, Shanghai 200093, China; Shanghai Key Laboratory of Multiphase Flow and Heat Transfer in Power Engineering, University of Shanghai for Science and Technology, Shanghai 200093, China;* orcid.org/0000-0002-4927-8500; Email: liudunyu@usst.edu.cn

Huancong Shi − *Huzhou Institute of Zhejiang University, Huzhou, Zhejiang 31300, China; Environmental Science and Technology, University of Shanghai for Science and Technology, Shanghai 200093, China;* orcid.org/0000-0003-4333-4118; Email: hcshi@usst.edu.cn

Authors

Qiuqi Liu − *School of Energy and Power Engineering, University of Shanghai for Science and Technology, Shanghai 200093, China; Shanghai Key Laboratory of Multiphase Flow and Heat Transfer in Power Engineering, University of Shanghai for Science and Technology, Shanghai 200093, China*

Mingguo Ni − *School of Energy and Power Engineering, University of Shanghai for Science and Technology, Shanghai 200093, China; Shanghai Key Laboratory of Multiphase Flow and Heat Transfer in Power Engineering, University of Shanghai for Science and Technology, Shanghai 200093, China*

Kailong Xu − *School of Energy and Power Engineering, University of Shanghai for Science and Technology, Shanghai 200093, China; Shanghai Key Laboratory of Multiphase Flow and Heat Transfer in Power Engineering, University of Shanghai for Science and Technology, Shanghai 200093, China*

Jingjing Ma − *State Key Laboratory of High-Efficiency Utilization of Coal and Green Chemical Engineering, College of Chemistry and Chemical Engineering, Ningxia University, Yinchuan, Ningxia 750021, China*

Zhuang Liu − *School of Energy and Power Engineering, University of Shanghai for Science and Technology, Shanghai 200093, China; Shanghai Key Laboratory of Multiphase Flow and Heat Transfer in Power Engineering, University of Shanghai for Science and Technology, Shanghai 200093, China*

Jing Jin − *School of Energy and Power Engineering, University of Shanghai for Science and Technology, Shanghai 200093, China; Shanghai Key Laboratory of Multiphase Flow and Heat Transfer in Power Engineering, University of Shanghai for Science and Technology, Shanghai 200093, China;* orcid.org/0000-0002-1681-9681

Complete contact information is available at: https://pubs.acs.org/10.1021/acsomega.2c01709

Notes

The authors declare no competing financial interest.

ACKNOWLEDGMENTS

This research was funded by the Natural Science Foundation of Shanghai (Project No. 21ZR1444400), the National Natural Science Foundation of China (Project Nos. 51706143 and 51976129), and the Foundation of State Key Laboratory of High-efficiency Utilization of Coal and Green Chemical Engineering (Grant No. 2022-K38).

REFERENCES

(1) Durmaz, M.; Dilmaç, N.; Dilmaç, Ö. F. Evaluation of performance of copper converter slag as oxygen carrier in chemical-looping combustion (CLC). *Energy* **2020**, *196*, No. 117055.

(2) Adánez-Rubio, I.; Nilsson, A.; Izquierdo, M. T.; Mendiara, T.; Abad, A.; Adánez, J. Cu-Mn oxygen carrier with improved mechanical resistance: Analyzing performance under CLC and CLOU environments. *Fuel Process. Technol.* **2021**, *217*, No. 106819.

(3) Alalwan, H. A.; Alminshid, A. H. CO_2 capturing methods: Chemical looping combustion (CLC) as a promising technique. *Sci. Total Environ.* **2021**, *788*, No. 147850.

(4) Cui, Z.; Li, Z.; Zhang, Y.; Wang, X.; Li, Q.; Zhang, L.; Feng, X.; Li, X.; Shang, L.; Yao, Z. Atmospheric mercury emissions from residential coal combustion in Guizhou Province, Southwest China. *Energy Fuels* **2019**, *33*, 1937−1943.

(5) Shahzad, N.; Hussain, A.; Mustafa, N.; Ali, N.; Kanoun, M. B.; Goumri-Said, S. First principles study of the adsorption and dissociation mechanisms of H_2S on TiO_2 anatase (001) surfaces. *RSC Adv.* **2016**, *6*, 7941−7949.

(6) Geng, X.; Duan, Y.; Zhao, S.; Xu, Y.; Ren, S.; et al. Study on mercury removal performance of mechanical-chemical brominated coal-fired fly ash. *Energy Fuels* **2019**, *33*, 6670−6677.

(7) Meng, J. L.; Duan, Y. F.; Hu, P.; et al. Simultaneous removal of elemental mercury and NO from simulated flue gas at low temperatures over Mn−V−W/TiO_2 catalysts. *Energy Fuels* **2019**, *33*, 8896−8906.

(8) Shen, F.; Liu, J.; Dong, Y.; Wu, D.; Gu, C.; Zhen, Z. Elemental mercury removal from syngas by porous carbon-supported $CuCl_2$ sorbents. *Fuel* **2019**, *239*, 138−144.

(9) Weng, X.; Mei, R.; Shi, M.; Kong, Q.; Liu, Y.; Wu, Z. $CePO_4$ catalyst for elemental mercury removal in simulated coal-fired flue gas. *Energy Fuels* **2015**, *29*, 3359−3365.

(10) Xing, L.; Xu, Y.; Zhong, Q. Mn and Fe modified fly ash as a superior catalyst for elemental mercury capture under air conditions. *Energy Fuels* **2012**, *26*, 4903−4909.

(11) Zhou, Q.; Lei, Y.; Liu, Y.; Tao, X.; Wang, Y.; et al. Gaseous elemental mercury removal by magnetic Fe−Mn−Ce sorbent in simulated flue gas. *Energy Fuels* **2018**, *32*, 12780−12786.

(12) Yan, J.; Jiao, H.; Chu, X.; Lei, Z.; Kang, S.; Li, Z.; Wang, Z.; Ren, S.; Shui, H. Investigation of potassium and copper decorations of Carajás hematite on coal-fuelled chemical looping combustion performance. *Fuel* **2021**, *286*, No. 119382.

(13) Ma, J.; Tian, X.; Zhao, B.; Li, X.; Zhao, Y.; Zhao, H.; Zheng, C. Behavior of mercury in chemical looping with oxygen uncoupling of coal. *Fuel Process. Technol.* **2021**, *216*, No. 106747.

(14) Wang, P.; Howard, B.; Means, N. Investigation of reactivities of bimetallic Cu-Fe oxygen carriers with coal in high temperature in-situ gasification chemical-looping combustion (iG-CLC) and chemical-looping with oxygen uncoupling (CLOU) using a fixed bed reactor. *Fuel* **2021**, *285*, No. 119012.

(15) Xu, K.; Liu, D.; Feng, L.; Jin, J.; Xiong, Z.; Ni, M.; Liu, Z.; Liu, Q.; Hou, F. Mercury removal by Co_3O_4@TiO_2@Fe_2O_3 magnetic

https://doi.org/10.1021/acsomega.2c01709
ACS Omega 2022, 7, 20959−20967

core-shell oxygen carrier in chemical-looping combustion. *Fuel* **2021**, *306*, No. 121604.
(16) Mendiara, T.; Izquierdo, M. T.; Abad, A.; de Diego, L. F.; García-Labiano, F.; Gayán, P.; Adánez, J. Release of pollutant components in CLC of lignite. *Int. J. Greenhouse Gas Control* **2014**, *22*, 15−24.
(17) Mendiara, T.; Izquierdo, M. T.; Abad, A.; Gayán, P.; García-Labiano, F.; de Diego, L. F.; Adánez, J. Mercury release and speciation in chemical looping combustion of coal. *Energy Fuels* **2014**, *28*, 2786−2794.
(18) Pérez-Vega, R.; Adánez-Rubio, I.; Gayán, P.; Izquierdo, M. T.; Abad, A.; García-Labiano, F.; de Diego, L. F.; Adánez, J. Sulphur, nitrogen and mercury emissions from coal combustion with CO_2 capture in chemical looping with oxygen uncoupling (CLOU). *Int. J. Greenhouse Gas Control* **2016**, *46*, 28−38.
(19) Ma, J.; Mei, D.; Tian, X.; Zhang, S.; Yang, J.; Wang, C.; Chen, G.; Zhao, Y.; Zheng, C.; Zhao, H. Fate of mercury in volatiles and char during in situ gasification chemical-looping combustion of coal. *Environ. Sci. Technol.* **2019**, *53*, 7887−7892.
(20) Ji, L.; Wang, Q.; Zhang, Z.; Wu, H.; Zhou, C.; Yang, H. Release characteristics of mercury in chemical looping combustion of bituminous coal. *J. Environ. Sci.* **2020**, *94*, 197−203.
(21) Gao, Y.; Zhang, Z.; Wu, J.; Duan, L.; Umar, A.; Sun, L.; Guo, Z.; Wang, Q. A critical review on the heterogeneous catalytic oxidation of elemental mercury in flue gases. *Environ. Sci. Technol.* **2013**, *47*, 10813−10823.
(22) Liu, Z.; Liu, D.; Jin, J.; Feng, L.; Ni, M.; Zhao, B.; Wu, X. Impact of gas impurities on the Hg^0 oxidation on high iron and calcium coal ash for chemical looping combustion. *Environ. Sci. Pollut. Res.* **2021**, *28*, 46130−46146.
(23) Ni, M.; Liu, D.; Jin, J.; Feng, L.; Liu, Z. Ranking oxygen carriers for elemental mercury oxidation in coal-fired chemical-looping combustion: A thermodynamic approach. *Energy Fuels* **2020**, *34*, 2355−2365.
(24) Zhou, J.; Luo, Z.; Hu, C.; Cen, K. Factors impacting gaseous mercury speciation in postcombustion. *Energy Fuels* **2007**, *21*, 491−495.
(25) Sliger, R. N.; Kramlich, J. C.; Marinov, N. M. Towards the development of a chemical kinetic model for the homogeneous oxidation of mercury by chlorine species. *Fuel Process. Technol.* **2000**, *65−66*, 423−438.
(26) Bale, C. W.; Bélisle, E.; Chartrand, P.; Decterov, S. A.; Eriksson, G.; Gheribi, A. E.; Hack, K.; Jung, I. H.; Kang, Y. B.; Melançon, J.; Pelton, A. D.; Petersen, S.; Robelin, C.; Sangster, J.; Spencer, P.; Van Ende, M. A. Reprint of: FactSage thermochemical software and databases, 2010−2016. *Calphad* **2016**, *55*, 1−19.
(27) An, M.; Ma, J.; Guo, Q. Transformation and migration of mercury during chemical-looping gasification of coal. *Ind. Eng. Chem. Res.* **2019**, *58*, 20481−20490.
(28) Wilcox, J.; Rupp, E.; Ying, S. C.; Lim, D.-H.; Negreira, A. S.; Kirchofer, A.; Feng, F.; Lee, K. Mercury adsorption and oxidation in coal combustion and gasification processes. *Int. J. Coal Geol.* **2012**, *90−91*, 4−20.
(29) Widmer, N. C.; West, J.; Cole, J. A. *93rd Annual Meeting*, In Thermochemical study of mercury oxidation in utility boiler flue gases; Air & Waste Management Association: Salt Lake City, Utah, 2000; p 2000.

https://doi.org/10.1021/acsomega.2c01709
ACS Omega 2022, 7, 20959−20967